A Comparative Analysis of the Fluid-Structure Interaction Method and the Constant Added Mass Method for Ice-Structure Collisions

Ming Song [a*], Ekaternia Kim [b, c, d], Jørgen Amdahl [b, c, d], Jun Ma [a], Yi Huang [a]

[a] *School of Naval Architecture and Ocean Engineering, Dalian University of Technology, Dalian, China*

[b] *Department of Marine Technology, Norwegian University of Science and Technology, Trondheim, Norway*

[c] *Centre for Autonomous Marine Operations and Systems (AMOS), NTNU, Norway*

[d] *Centre for Sustainable Arctic Marine and Coastal Technology (SAMCoT), NTNU, Norway*

*Corresponding author. Email: ming.song@ntnu.no

A Comparative Analysis of the Fluid-Structure Interaction Method and the Constant Added Mass Method for Ice-Structure Collisions

Two numerical methods which are constant added mass (CAM) method and fluid-structure interaction (FSI) method are widely used for simulating ship-ship and ship-ice collisions. In the CAM method, the hydrodynamic effect of the surrounding water is treated as a constant added mass, whereas in the FSI method the surrounding fluid flow is explicitly modelled. As there is a lack of analysis in the difference between the CAM method and the FSI method, there is a strong need for an investigation and comparison of the two methods. In this paper, to compare the methods, we considered a collision between a freshwater ice block and a floating steel structure. The numerical simulations were performed using two methods by LS-DYNA software. The behaviour of the ice was modelled using an elliptic yield criterion and a strain-based pressure-dependent failure criterion. To ensure get accurate results, the ice model was verified using empirical data from laboratory and in-situ indentation tests and the fluid model in the LS-DYNA was verified by comparing the added mass coefficients for a spherical body and a rectangular block with the corresponding WADAM results. To validate and benchmark the numerical simulations, experimental data on ice-structure interactions in water were used, including the acceleration of the floater wall with the dynamic motion unit (DMU) on it, the relative velocity between the ice and the floater before the impact and some images extracted from video recording of the test. The results of the comparisons indicated that the FSI method yielded better results for the motion of the floater, i.e., the acceleration of the floater wall caused by the ice block's impact and the relative velocity were in reasonably good agreement with experimental measurements. The results also indicated that the CAM method was faster but predicted a higher peak impact force and more dissipated energy in the ice block than the FSI method did.

Keywords: numerical simulation; fluid-structure interaction; constant added mass; ice-structure collision; freshwater ice

1. Introduction

Collisions with massive ice floes can directly result in the loss of human life, environmental damage and structure loss, and it is important to design engineering structures (i.e., bridges, ships and offshore structures) that have sufficient resistance to ice collisions (e.g., IACS [1] and DNV GL [2]). With the rapid development of computer technology in recent years, numerical simulations have been increasingly used in analyses of collisions between ice and ships to predict structural damage and to complement physical testing during the early stage of the design process (e.g., [3,4]). Experimental studies remain either very expensive or difficult to conduct.

The hydrodynamic effect of the surrounding water plays an important role in the analysis of ship-ship collisions, ship-platform collisions and collisions between ice and movable structures [5]. For instance, hydrodynamic forces cause a struck ship or floating body to move before the actual impact, which affects its response to the collision [6]. It is necessary to take into account of hydrodynamic effect of surrounding water in dealing with the absorbed energy by collision [7].

A review of studies of ice-structure collisions that use the finite element method reveals that there are two common methods of considering the hydrodynamic effects of the surrounding water in assessments of the amount of energy absorbed in platform-ice and ship-ice collisions. One is the *constant added mass* (CAM) method, in which the effect of the surrounding fluid is treated as a constant added mass, and the other is the *fluid-structure interaction* (FSI) method, in which the surrounding fluid is explicitly modelled. However, only few studies have focused on the difference between the CAM method and the FSI method with respect to the energy dissipated during a collision. As a contribution to knowledge, there is a strong need for an investigation and comparison of the two methods.

The objective of the present study is to compare the CAM and FSI methods for numerically simulating a collision between an ice block and a floating structure. To the authors’ knowledge, this is the first comparative analysis of these methods for ice-structure collision problems.

All the simulations described in this paper are performed by LS-DYNA. We address the FSI problem using an ALE formulation and an ALE to Lagrangian formulation coupling algorithm [8]. The modelling technique used with the FSI method is presented in detail. The focus is on validating the model's input parameters and the key numerical results using experimental data on freshwater ice-steel structure collisions. First, the ice model parameters and LS-DYNA's fluid model are validated. Second, the results of laboratory collision experiments in water are used to verify the FSI technique and to evaluate the two methods. Finally, the results of the two methods, including the acceleration of the floater wall with the dynamic motion unit (DMU) on it, the contact force, the energy dissipation and the central processing unit (CPU) time, are compared and discussed.

The layout of the paper is as follows: Section 2 describes the advantages and drawbacks of the CAM method and the FSI method; Section 3 presents the experimental data that were used for the validation and evaluation of the numerical models; Section 4 presents the details of the two methods, including the simulations' setup, validation and major results; Section 5 presents a comparison of the results obtained using the FSI and CAM methods; and Sections 6 and 7 present a discussion and the conclusions, respectively.

2. CAM method and FSI method

2.1. The CAM method

In a collision scenario, the analysis procedure is decoupled into two independent parts: the external dynamics and the internal mechanics. The external dynamics addresses the energy released for dissipation and the impact impulse of the collision by analysing the rigid motions of the colliding ships and by accounting for the effect of the surrounding water. The internal mechanics is concerned with how the strain energy is dissipated in the striking and struck objects. That these are decoupled implies that there is no interaction between the ships' motions and structural deformations. A simplified decoupled method for colliding ships was first presented by Minorsky [9]. In the force-acceleration relationship, he proposed using a constant value of 0.4 for the sway added mass coefficient of the struck ship, and since then, this value has been used in analyses of ship-ship and ship-ice collisions (see, e.g.,[10][11]).

Because of its simplicity, the CAM method has attracted the most attention in marine engineering. Within the framework of the decoupled method, the majority of ship-structure (or ice) collision problems have been solved using the CAM method (see Table 1). For the external dynamic analysis, the constant added masses of two impact bodies were widely used for accounting for the effect of the surrounding water in dealing with the energy dissipation and impact force by analytical method [12][13][14]. For the internal mechanic analysis, the constant added mass of the colliding body was usually included in the numerical simulations [15][16]. In the coupled method, Wang et al. [10] and Zhang et al. [17] used the CAM assumptions for finite element analysis of ship-ship collisions. However, most of them used the other simulations or some simplified formulations to validate their results and there is a lack of experiments to validate the CAM method immediately.

There are several limitations of the assumption of constant added mass. Those are:

1. In reality, the added mass of the struck ship depends both on the duration of the collision and on the relationship between the collision force and the deformation.

2. Using the CAM method means neglecting the effects of the presence and the motion of the other body during the approach and collision processes.

3. The effects of free-surface wave generation cannot be considered in the CAM method.

The first limitation indicates the "uncertainty" of the added mass. Motora et al. [7] investigated the validity of Minorsky's assumption of constant added mass in a series of model tests and concluded that this assumption is only reasonable when the duration of the collision is very short. For collisions with longer durations, the value of the added mass increases and can reach a value that is equal to or even greater than the ship's own mass. The second limitation represents a lack of the effect of the relative motion of the ice and the structure, and the third indicates that the time-varying wetted surfaces of the two bodies during the impact are neglected. These can have consequences for the accuracy of the fluid-structure interaction depending on the time scale of the impact and the geometries and kinematics involved.

2.2. The FSI method

In contrast to the decoupled CAM approach, the FSI approach can provide solutions to fully coupled ship collision problems in which the surrounding water flow is explicitly modelled and actual ship motions are considered in the evaluation of the contact forces. The solution is obtained using numerical methods such as computational fluid dynamics (CFD), the arbitrary Lagrangian Eulerian (ALE) method, smoothed-particle hydrodynamics (SPH) and other simplified fluid dynamical simulation methods (see, e.g., [18][19][20][21]).

Currently, the ALE method is most frequently used to analyse ship-ship and ship-ice collisions in which the FSI is explicitly considered. To solve a water-structure interaction problem, a Lagrangian formulation is adopted for the structural materials, and an ALE formulation is adopted for the water. In addition, with both Lagrangian and ALE formulations, a contact type algorithm is used to handle the coupling between the water and the structure's materials. This method is capable of coupling external and internal mechanics. Several research articles have presented results of FSI-based simulations that use LS-DYNA's ALE formulation (see Table 1). Therein, some of them are lack of validations for the FSI-based simulations of ship-rigid structure collision [22], ship-ship collision [6] and ship-iceberg collision [23]. Wang and Derradji [24] carried out wave-maker simulations using

ALE method to compare the wave length with the data used for calibration. However, the ship and the ice were treated as rigid bodies in the collision model, which decrease the reality and accuracy with respect to prediction of structural damage. Gagnon and Derradji [25] conducted an ALE simulation of a ship colliding with bergy bits. It showed a good agreement with the experiment in the sway motion. Gagnon and Wang [26] performed the numerical simulations of a collision between a bergy bit and a tanker using ALE formulation to incorporate hydrodynamics. Load measurements from the lab tests compared reasonably well with estimates from the simulation. However, the validation for the case of FSI analysis of ice-structure collision remains a topic of active research.

There are serval limitations for the ALE method in LS-DYNA:

1. It is predominantly applicable to laminar flow. Also, the ALE solver is not a full Navier-Stokes solver and thus does not account for fluid boundary layer effects such as drag. Effects of fluid viscosity derive solely via the material model [ ].

2. It computes the coupling force using a penalty method, i.e., the force is always a function of the displacement. While in reality, the added mass is in phase with acceleration or deceleration.

3. This fully coupled ALE method requires considerable modelling efforts and large computation resources.

Table 1. Summary of the previous studies on ship-structure collision and ice-structure collision

Source	Collision problem considered	Tool	Water representation	Modeled phenomenon	Validation
Pedersen and Zhang [12]	Ship-ship Ship-rigid wall Ship-offshore structure	Analytical	CAM	Energy loss	Compared energy loss with that calculated by time domain simulation
Yamada and	Ship-ship	Analytical	CAM	Force and energy	Compared force and

Pedersen [13]					energy with those obtained by FEA
Yang and Caldwell [14]	Ship-bridge pier	Analytical	CAM	Force and collision duration	Compared the crushing strength of the bow with Minorsky's formula and Gerard's formula
Kim et al. [15]	Ship-ice masses	LS-DYNA	CAM	Impact force, motion of the plate and plate deflection	Compared the force and plate deflection with data from the test
Kwak et al.[16]	Ship-ice	MSC/DYTRAN	CAM	Strength of bow structure and mechanical properties of ice	Compared with ice design load for IACS Polar Class Rules
Wang et al. [10]	Ship-ship	MSC/DYTRAN	CAM	Contact force and energy	None
Zhang and Suzuki [17]	Ship-ship	LS-DYNA	CAM for surrounding water and FSI for crude oil inside the tank	Energy, motion and impact force	Compared pressure and impulse with data from a drop experiment
Derradji and Earle [22]	Ship-structure	LS-DYNA	FSI	Motion and stress	None
Lee et al. [6]	Ship-ship	LS-DYNA	FSI	Damage configuration	None
Lee and Nguyen [23]	Ship-iceberg	LS-DYNA	FSI	Motion	None
Wang and Derradji [24]	Ship-ice floe	LS-DYNA	FSI	Contact force	Compared the wave details with data used for the calibration
Gagnon and Derradji [25]	Ship-bergy bit	LS-DYNA	FSI	Sway displacement, load and pressure	Compared the sway motion with the data in the field

Gagnon and Wang [26]	Ship-iceberg	LS-DYNA	FSI	Load and pressure	Compared the load with lab data

3. Experimental data

This section reports the experimental data that are used for validation and to test the effectiveness of the CAM and FSI methods. Data collected from ice-structure indentation and impact tests are considered. Pressure-area data from laboratory and *in-situ* tests on freshwater ice at constant and variable indentation speeds are used to quantify the degree to which the ice model accurately represents the failure process of ice during a collision. The results of laboratory experiments on collisions between ice and a movable steel structure are used to verify the FSI technique and to quantify the confidence in and predictive accuracy of the FSI and CAM methods.

3.1 Ice indentation and impact data

Indentation and impact tests provide force-time plots that are converted to pressure-area data. Figure 1 presents the pressure-area data collected using freshwater laboratory-grown granular ice (see [3] and [18-20]) and natural iceberg ice [21] on millimetre and metre scales. Using a lower bound estimate of these experimental data from freshwater granular ice, an empirical pressure-area relationship ($P = 0.35A^{-0.5}$) was determined (see Figure 1). This relationship serve as a basis for building credibility in the constitutive model of ice and for validating the input parameters for ice. In the interest of clarity, we limit ourselves to the tests in which the ice exhibited characteristics of brittle compressive failure such as radial cracks, spalling, saw-tooth loading, etc.

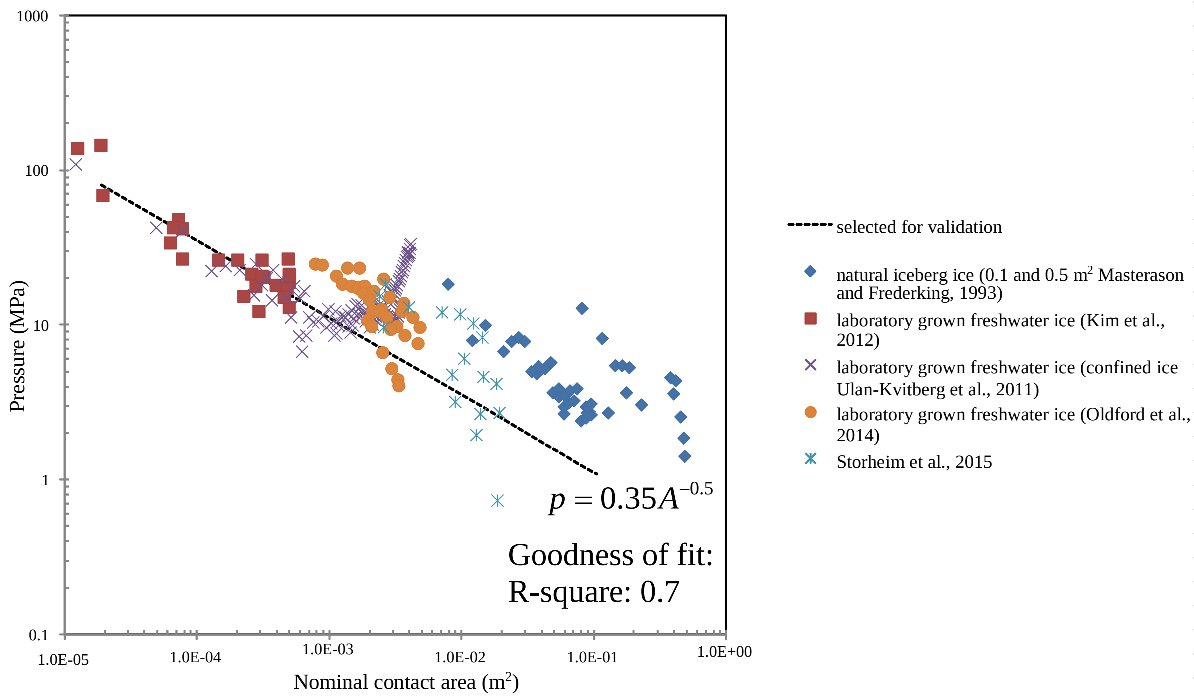

Figure 1. A pressure-area log-log plot: $p = 0.35A^{-0.5}$ is a lower bound pressure estimate for spherical rigid indenter.

3.2 Ice-structure collision data

This section presents experimental data that are used to verify the FSI technique and to evaluate the CAM and FSI methods. Detailed information about the experiments can be found in Kim et al. [13]. Only a short summary is presented here. The interaction between an ice block and a stationary floating structure in water was considered. The tests were conducted at the Aalto ice tank facility using laboratory-grown freshwater granular ice and a steel floating structure. The test represents impacts between an approximately 1000-kg ice block and a purpose-built steel target at speeds of 1.0 and 2.0 m/s (Figure 2). A total of 18 impact tests were conducted. Test no. 11 was selected for the analysis because it represents a central impact most accurately. In this test, the ice block's mass was 850 kg and the impact speed was approximately 2.0 m/s.

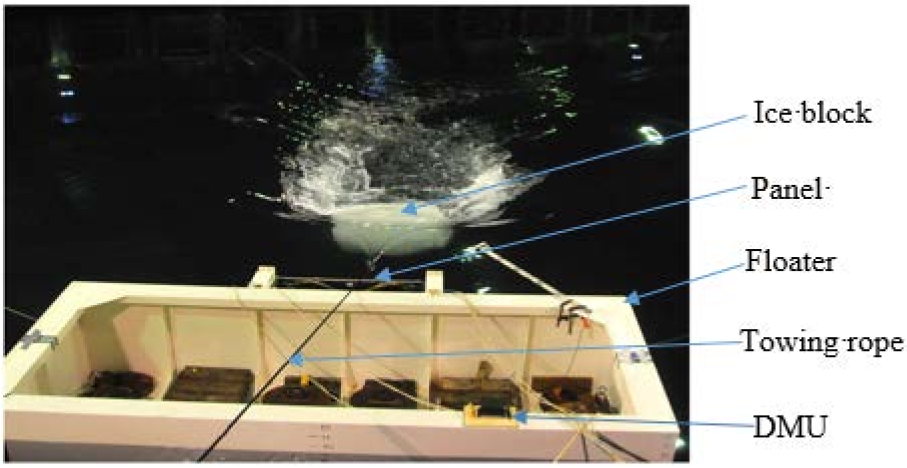

Figure 2. Photograph of a typical impact event. The floater carries a dynamic motion unit (DMU) to record its acceleration.

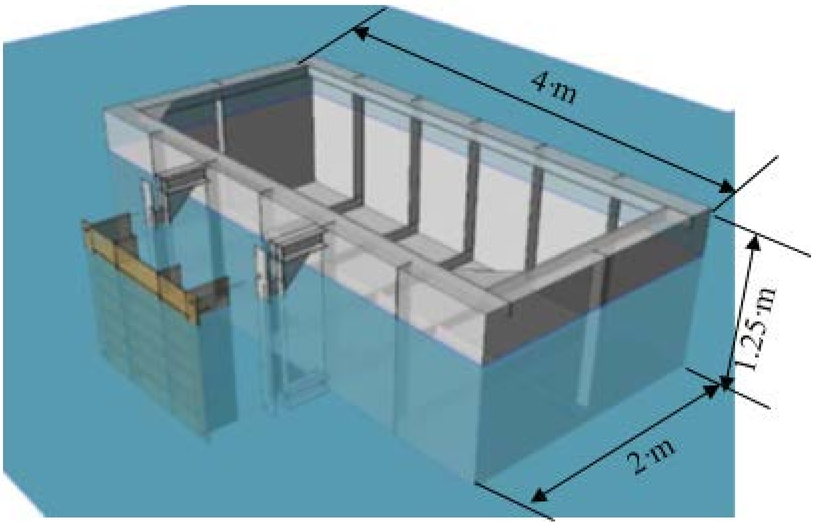

(a)

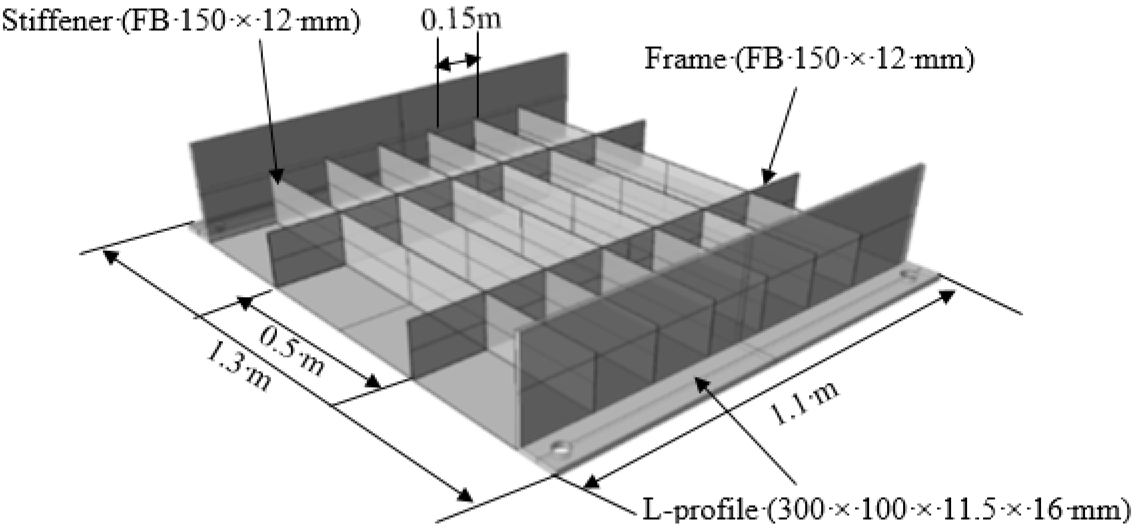

(b)

(c)

Figure 3. The geometry of the impacted structure and the ice block: a- the scheme for attaching a stiffened panel to the floater; b- a stiffened panel (mild steel); and c- the freshwater ice block (the grid lines are 0.15 m apart).

Figure 3 shows the geometry of the impacted structure and the ice block. The structure consisted of a stiffened panel bolted to a floater. The global dimensions of the floater at the water plane were 2 m × 4 m, its draught was 0.95 m and its total height was 1.25 m. The total weight of the floater including the 12-mm thick impact panel was 7537 kg. The overall dimensions of the panel were 1.1 m × 1.3 m. The panel was supported by six transverse flat-bar stiffeners; they were 150 mm high and placed 500 mm apart, as shown in Figure 3 (b). The total plate area of 1100 mm× 1100 mm (excluding the L-profiles) was wider than the expected area of crushed ice. The ice block had overall dimensions of 1.0 m × 1.2 m and a height of 0.9 m, as shown in Figure 3 (c).

The impact event was recorded using a high-speed video (HSV) camera and five video cameras at different angles. A dynamic motion unit (DMU) recorded the acceleration of the floater using a data acquisition system with a sampling frequency of 523 Hz. The floater's acceleration, the HSV images and the velocity of the floater (and the ice block) are used for validating and evaluating the numerical results.

4. Numerical analysis

This section details the FSI and CAM methods, including the simulation setup, the model validation process and major results.

4.1. The FSI method

4.1.1 Simulation setup

Figure 4 shows the numerical domain of the simulations. It consisted of water, air, the floater and a spherical ice block. The dimensions of the modelled region were 12 m × 10 m × 4 m, including 1.5 m air on the top. The dimensions of the floater are shown in Figures 3 (a) and 3 (b). For simplicity, the ice block shown in Figure 3c was assumed to be a sphere with radius R = 0.61 m. The coordinate system is also shown in Figure 4, in which the direction of the ice block's forward motion (i.e., the impact direction) was defined as Y-axis. In this paper, the motions of the ice block and the floater in the Y-direction were assumed as sway motions.

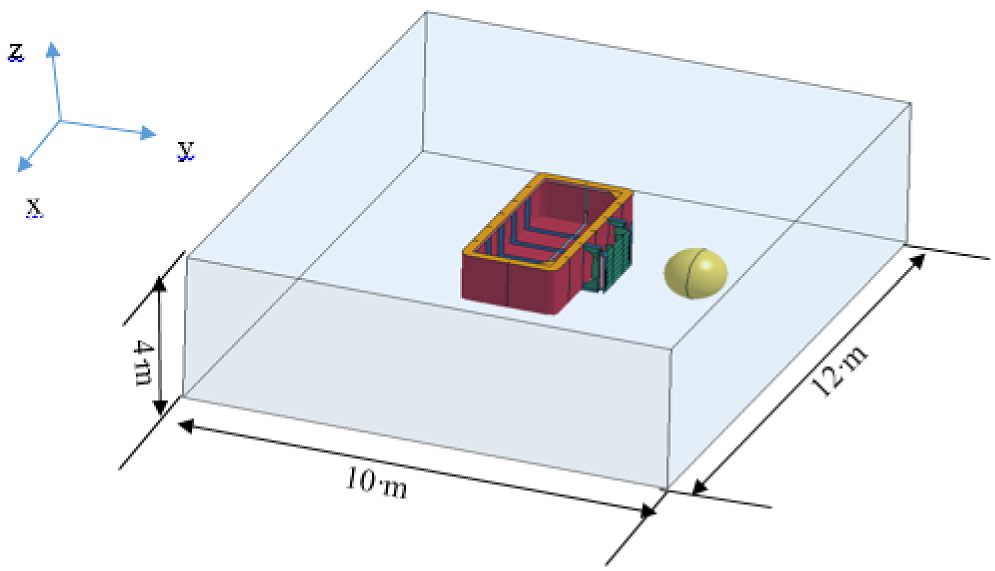

Figure 4. The meshed region for the ice block and floater collision simulations.

The hydrostatic pressure was simulated using the procedure described by Day [22]. The air and water were modelled using eight-node solid elements with a one point ALE multi-material element formulation (by tracking the interface of the two materials within each element). The mesh size for the air and water was100 mm × 100 mm × 100 mm. The ice block and floater were discretized using Lagrangian-based finite element formulations, i.e., eight-node solid elements with reduced integration for the ice and four-node Belyscho-Tsay shell elements with 5 integration points along the thickness for the floater. The mesh size for the ice block was approximately 12 mm × 12 mm × 12 mm. To reduce the computation time, the rear half of the ice block was meshed with rigid brick elements because it was relatively far from the impact area. The floater was meshed with an element size of 30 mm.

The Lagrangian mesh was allowed to overlap the ALE mesh and the two meshes interacted according to LS-DYNA's coupling algorithm [23]. This coupling served to generate forces that resisted penetration of the ALE mesh into the Lagrangian mesh.

To avoid numerical errors caused by overlapping meshes, we ensured that the water was removed from the volume that was occupied by the objects when the ice block model and the floater model were added to the LS-DYNA k-file.

The ice block travelled through a distance of 1.0 m to allow a head wave to develop before the collision; this avoided having it traverse an overly large volume of water, which would have necessarily increased the simulation time substantially. The contact between the ice block and the plate was implemented using a contact-eroding surface-to-surface formulation, which was used with the segment-based contact option (soft=2). The contact force between them was contained in the ‘rcforc’ file produced by using a database-rcforc command. The self-contact of the ice component was implemented using the contact-eroding single-surface formulation with a static coefficient of friction of 0.15.

The behaviour of the ice (except for the rigid part) was modelled using the elliptic yield criterion and the strain-based pressure-dependent failure criterion for freshwater granular ice implemented by Liu et al. [24]. The model is dependent on the hydrostatic pressure, and thereby the triaxial loading state of the ice. A Tsai-Wu yield surface was fitted to experimental data sets. The yield surface is a function of both the second invariant of the deviatoric stress tensor J_2 and the hydrostatic pressure p as

$$f(p, J_2) = J_2 - (a_0 + a_1 p + a_2 p^2) = 0 \tag{1}$$

with coefficients a_0, a_1 and a_2. When an element reaches plasticity in compression, it follows the yield surface until failure. Due to low tension capacity of ice, an element is removed by erosion if the tensile stress surpass 2 MPa. For compressive stress-states, failure by element erosion was activated if the equivalent plastic strain ε_{eq} (compressive) reaches the failure curve ε_f, defined by

$$\varepsilon_f = \varepsilon_0 + (\frac{p}{p_2} - 0.5)^2 \qquad (2)$$

In which ε_0 is the initial failure strain and p_2 is the larger root of the yield function (Eq.1). The Tsai-Wu criterion is plotted in Figure 5. This failure criterion is based on trial and error and is purely empirical. For details, please refer to work by Liu et al. [24].

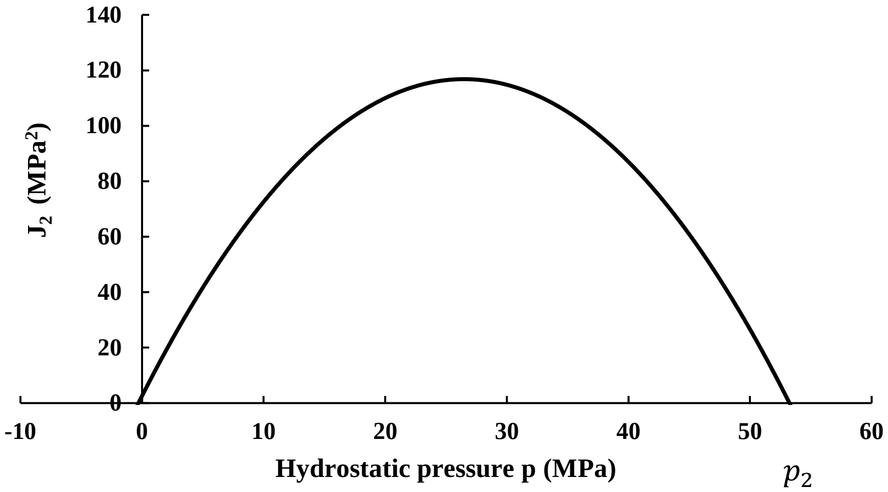

(a) Yield surface

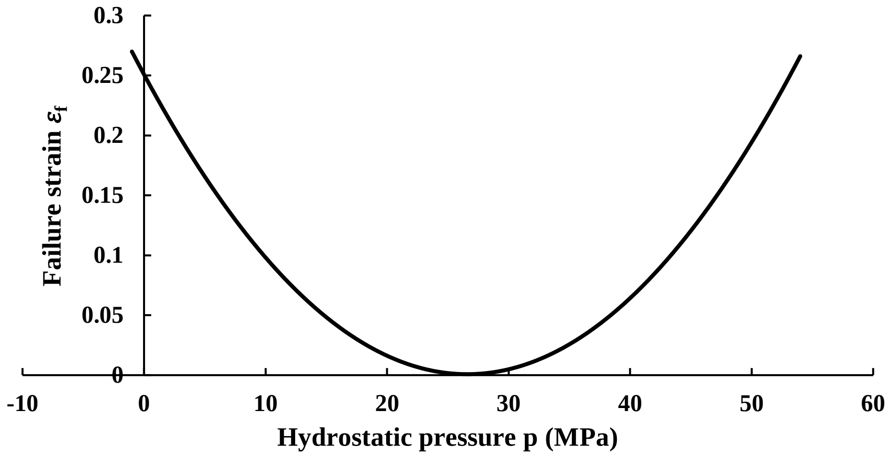

(b) Erosion criteria

Figure 5. Tsai-Wu yield surface and erosion limit with the parameters used herein (see Table 2).

For the steel, the model implemented and verified by Alsos et al. [25] was used; it incorporated a plateau strain, power law hardening and RTCL damage criterion. The equivalent stress-strain relationship is:

$$\sigma_{eq} = \begin{cases} \sigma_y & \text{if } \varepsilon_{eq} \le \varepsilon_{plat} \\ K(\varepsilon_{eq} + \varepsilon_0)^n & \text{otherwise} \end{cases} \tag{3}$$

where ε_{plat} is the equivalent plastic strain at the plateau exit and σ_y denotes the initial yield stress, *K* is strength index, *n* is the strain hardening index. The strain ε_0 at the intersection of the plateau and power law expression, $(\varepsilon_{plat}, \sigma_y)$ is given by the following expression:

$$\varepsilon_0 = (\frac{\sigma_y}{K})^{\frac{1}{n}} - \varepsilon_{plat} \tag{4}$$

The RTCL damage criterion was employed. Detailed information can be found in the paper by Also et al.[ ].The material parameters used for the ice block and the floater are listed in Table 2.

Table 2. Material parameters used in the FSI-based numerical simulations.

Ice parameter used in Liu's model	Value	Mild steel parameter	Value
Ice density (kg/m^3)	900	Steel density (kg/m^3)	7890
Young's modulus (GPa)	9.5	Young's modulus (GPa)	210
Poisson's ratio (-)	0.3	Poisson's ratio (-)	0.3
Inelastic a_0 (MPa^2)	2.588	Yield stress (MPa)	235
Inelastic a_1 (MPa)	8.63	Strength index *K* (MPa)	700
Inelastic a_2 (-)	-0.163	Strain index *n* (-)	0.24
Initial failure strain (-)	0.008	Initial failure strain (-)	0.005

Ice-steel friction (-)	0.15	Mesh exponent (-)	0.71

4.1.2 Verification of the material model of ice

Because small changes in the ice input data may cause significant changes in the outcome in terms of structural deformations and energy dissipation [24], it is essential to verify that the material model of ice is capable of predicting a reasonable pressure-area relationship that is in agreement with the experimental data for freshwater ice (in Section 3.1).

A numerical simulation of a collision between the freshwater ice block and a rigid plate was performed. The ice's geometry and material parameters were the same as those used in the FSI-based simulation described in Section 4.1.1. The mesh size for the rigid plate was approximately 30 mm × 30 mm. For the ice block, to check the solution's convergence, four meshes with characteristic element lengths of 20 mm, 15 mm, 12 mm and 10 mm were considered.

The results of the simulation are presented in terms of the average pressure versus the nominal contact area in Figure 6. The ice pressure was calculated by dividing the contact force by the nominal contact area, which is a function of the penetration distance. For comparison purposes, the empirical pressure-area relationship ($P = 0.35A^{-0.5}$) which was determined by the model's predictions with the experimental data for laboratory-grown freshwater ice within the brittle regime (i.e., see Section 3.1) is also plotted. Two points are noteworthy: first−figure 6 shows that convergence is reached when the element size is smaller than 15 mm: the results from the element size of 12 mm and 10 mm are very close. A trade-off between computation time and accuracy supports a mesh size of 12 mm. Second−there is a good agreement between the simulation results and the empirical ice pressure-area relationship when the element size of the ice block is smaller than 15 mm. The results of numerical simulations indicate that the material model of ice (including the input parameters) with the element size of 12 mm is able to predict accurate results with respect to the pressure-area relationship.

For natural iceberg ice or other types of ice, one can improve the predictive accuracy of the ice model by additional tuning of the model parameters listed in Table 2.

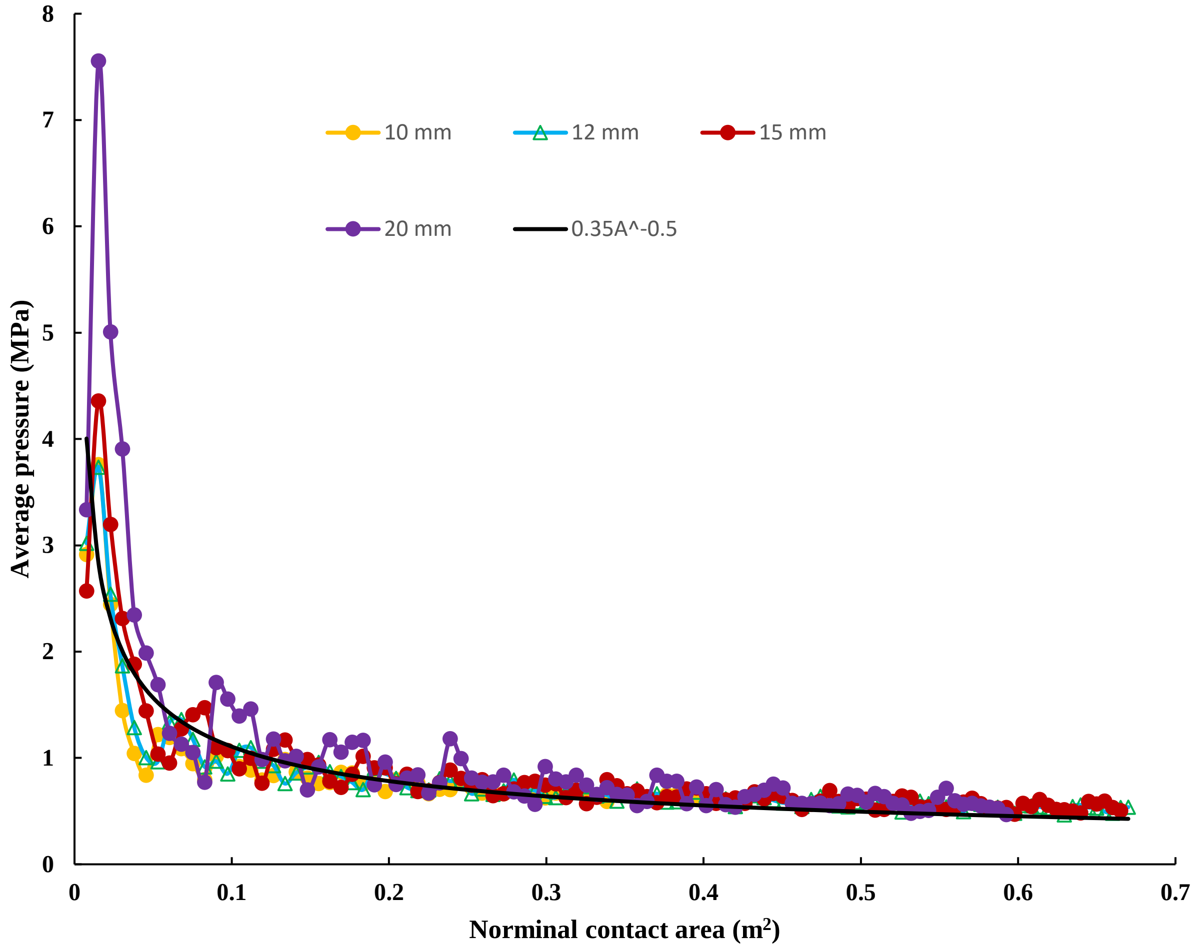

Figure 6. The average contact pressure versus the nominal contact area.

4.1.3 Verification of LS-DYNA's fluid model

Performing an ALE analysis with LS-DYNA is not straightforward, and it is important to verify that the fluid model provides accurate results. One way to verify the model is to calculate the equivalent added mass coefficients of the floater (a rectangular box) and the ice block (a sphere) and then, to compare them with the values obtained using the potential flow solver WADAM.

The frequency-dependent added mass of each object was found using the following procedure: the geometry of each object was the same as it was in the test, and the material was assumed to be rigid. The densities were adjusted to obtain the draft used in the test. The objects swayed freely and were restrained in all other DOFs. Each object was made to oscillate by applying a harmonic sway force history (in the y-direction) (see Figure 7). Using the time histories for the acceleration and displacement of the floater and the ice block, the added mass was calculated for a range of frequencies between 12 and 50 rad/s, which were considered representative of the impact situation.

The harmonic excitation force was applied for five periods for each frequency. The frequency-dependent added mass was found using Eq. 1, which applies when the displacement reaches a maximum, the velocity of the object is zero, and the only contribution to the dynamic equilibrium is the inertial force.

$$(M + A_{yy})\ddot{y} = F_y(t) \tag{5}$$

Here, M is the mass of the object, A_{yy} is the added mass in the sway direction induced by the acceleration in the y-direction and $F_y(t)$ is the excitation force in the y-direction. $\ddot{y}$ is the acceleration of the object in the sway direction.

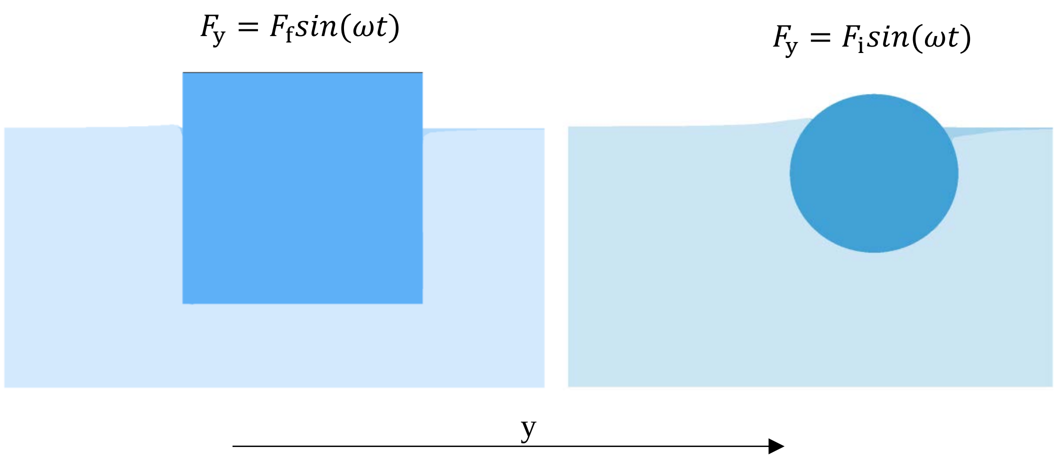

Figure 7. Side view: The floater (left) and ice (right) were made to oscillated for the estimation of the added mass coefficients.

Figure 8 shows results of the simulations in which the external force was approximately 10 times the floater's weight at a frequency of 21 rad/s.

To assess the effect of the magnitude of the force, four different amplitudes for both the floater and the ice block were used in the simulations performed at a frequency of 21 rad/s. The results are shown in Figure 9 and Figure 10. It is observed that the sway added masses of the floater and the ice are virtually independent of the magnitude of the force in this analysis.

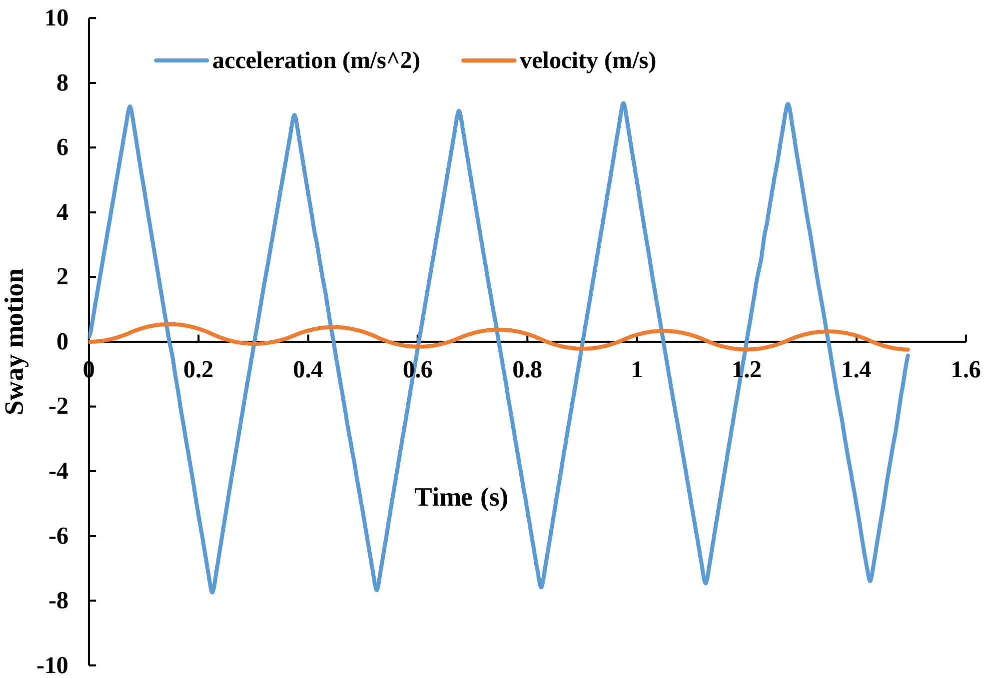

Figure 8. The time history of the floater's sway motion.

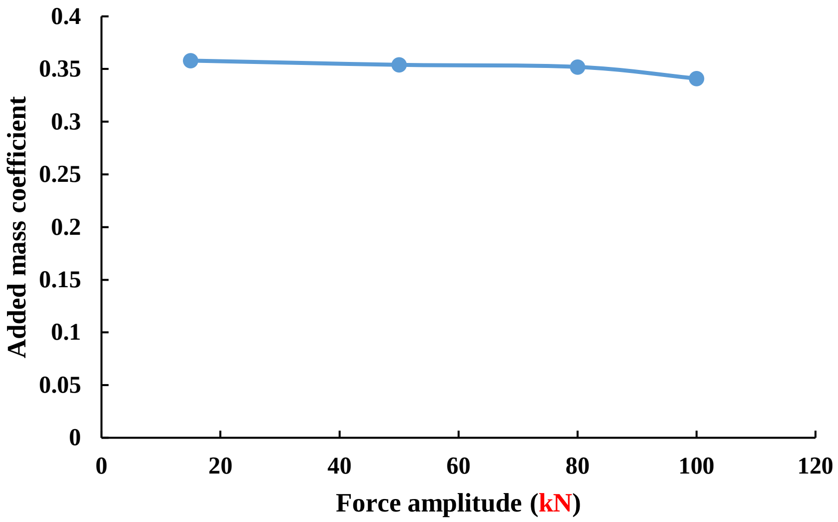

Figure 9. The influence of the magnitude of the force on the sway added mass coefficient for the floater (the added mass coefficient is the ratio of the added mass to the mass of the body).

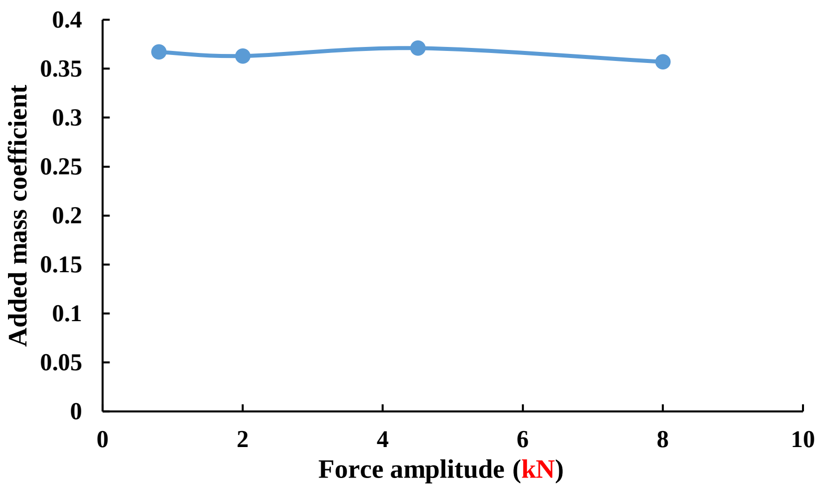

Figure 10. The influence of the magnitude of the force on the sway added mass coefficient for the ice

Figure 11 and Figure 12 present the results of the LS-DYNA simulations with the added mass coefficients calculated by WADAM for frequencies between 12 and 50 rad/s.

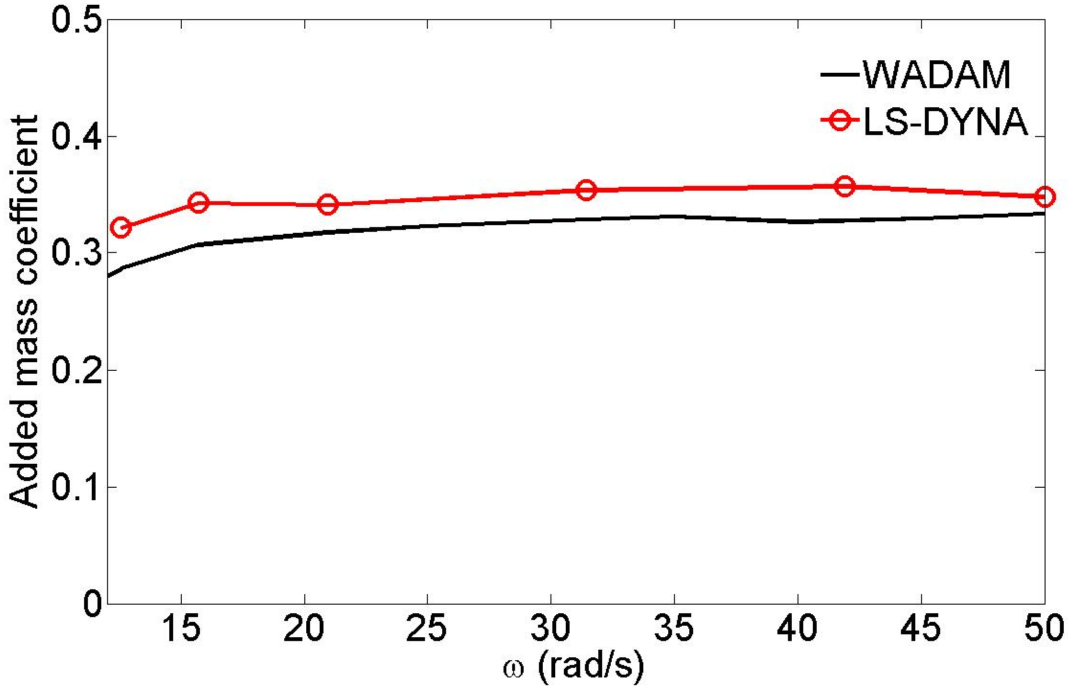

Figure 11. A comparison of the added mass coefficients from LS-DYNA and WADAM for the floater (ω is the frequency).

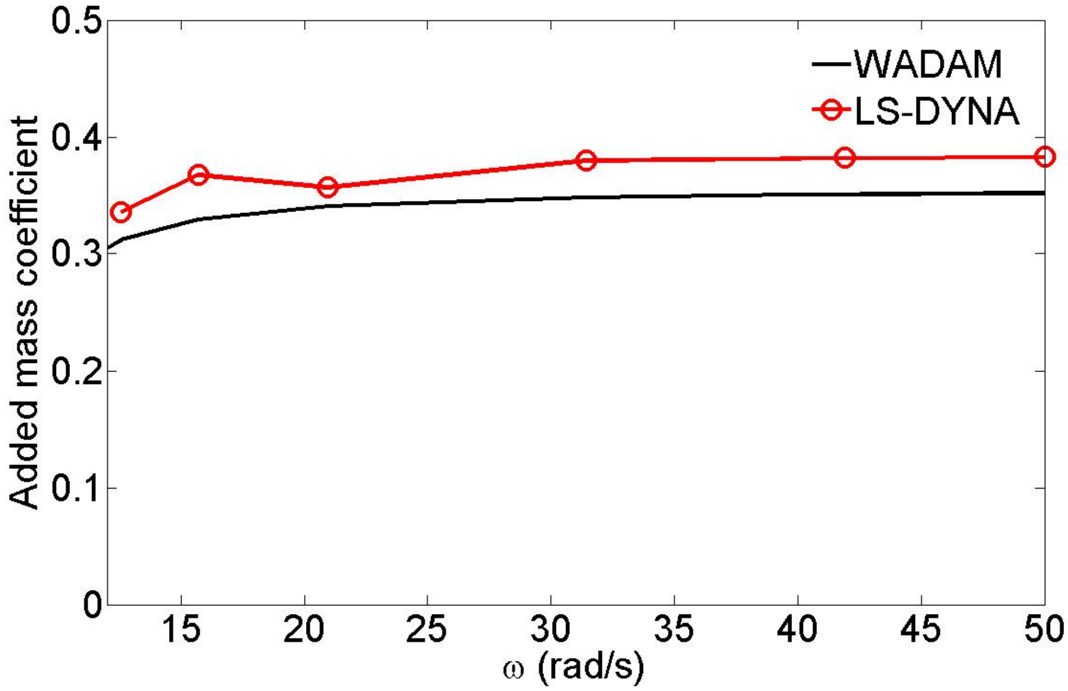

Figure 12. A comparison of the added mass coefficients from LS-DYNA and WADAM for the spherical ice block (ω is the frequency).

The comparisons of the results show that the added masses of both the floater and the ice block calculated using LS-DYNA are very close to the values obtained using WADAM for high frequencies ($\omega \geq 10$ rad/s). For the floater, the added mass coefficient for infinite high frequency was approximately 0.35 in the LS-DYNA simulation, compared to 0.33 in the WADAM simulation. For the ice block, the added mass coefficient for infinite high frequency was approximately 0.38 in the LS-DYNA simulation, compared to 0.35 in the WADAM simulation. These differences are most likely due to the nature of the fluid-structure coupling in DYNA which computes the coupling force using a penalty method, i.e., the force is always a function of the displacement. While in reality, the added mass is in phase with acceleration or deceleration. WADAM uses widely accepted linear frequency domain methods for marine hydrodynamics. The frequency dependent added mass is calculated based on potential theory. Results using WADAM are more trustworthy [ ].

Overall, it is concluded that a collision analysis performed using the FSI technique in LS-DYNA may give realistic results as far as the added mass is concerned. The values calculated by WADAM were used for CAM method.

4.1.4 Verification of the FSI technique for analysing ice-structure collisions

This section presents a mesh conversion of study and comparisons between the results of the FSI-based simulations and the results of the laboratory experiments, including pictures of the collision and the relative velocity between the floater and the ice block before the impact. It is noted that the input parameters of the material model of ice and the FSI method were measured in physical and numerical experiments (see Sections 3.1.2 and 3.1.3) and are independent of the tests used to validate the accuracy of the FSI method.

The mesh conversion study was carried out by comparing the time histories of the contact forces. Figure 13 shows that the peak of the contact force decreases with reducing the mesh size. It is found that the contact force is sensitive to the mesh size both in terms of oscillation amplitude and period. There is little difference in contact force between case II and case III. Therefore, 12 mm for the ice block and 30 mm for the floater are then considered as an appropriate element size for subsequent simulations.

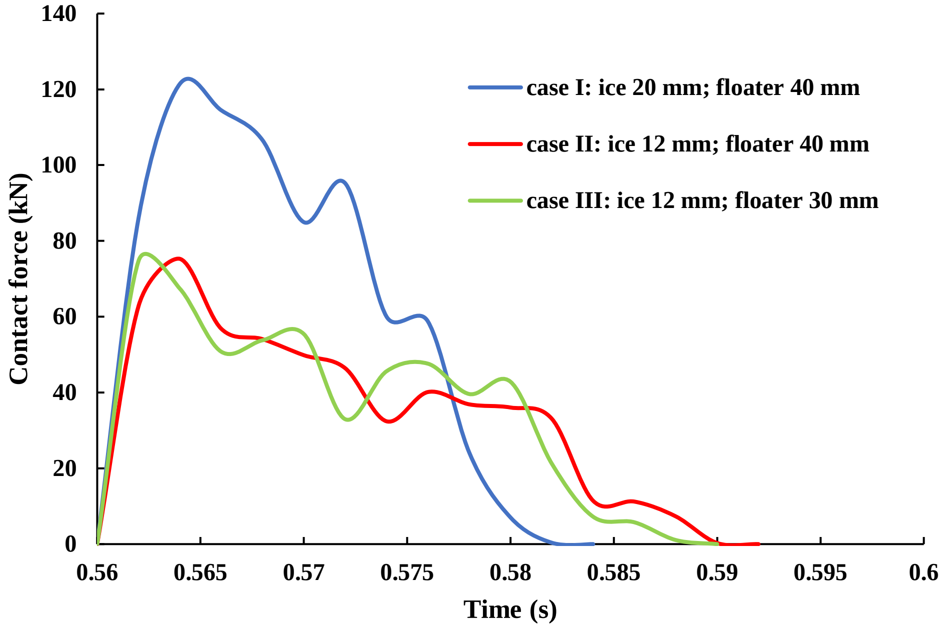

Figure 13. Contact force for different mesh sizes

Figure 14 and Figure 15 show images extracted from video recordings of the test and from the FSI-based simulations. It is observed that the ice block generated a progressive disturbance (a bow wave) that caused water to pile up in front of the panel before the actual impact in the HSV of the test. The floater exhibited a lateral response to the bow wave in the test. A very slow drift of the floater in the direction of the impact occurred before the actual impact. This drift was caused by the water pile-up. Similar results were observed in the simulations.

The agreement between the tests and the FSI-based simulations of these phenomena is reasonably good. The velocities of the ice block and the floater before the impact were 1.9 m/s and 0.17 m/s in the FSI-based simulation, respectively, and 1.8 m/s and 0.1 m/s, respectively, in the test. These differences are not surprising because the velocity in the tests is the average velocity, which was estimated using a few images extracted from the high-speed video recordings after the impact. From the perspective of the velocity of the ice block relative to the floater, the FSI-based simulation agrees well with the test (the relative velocities before the impacts were 1.73 m/s and 1.70 m/s in the FSI-based simulation and the test, respectively.)

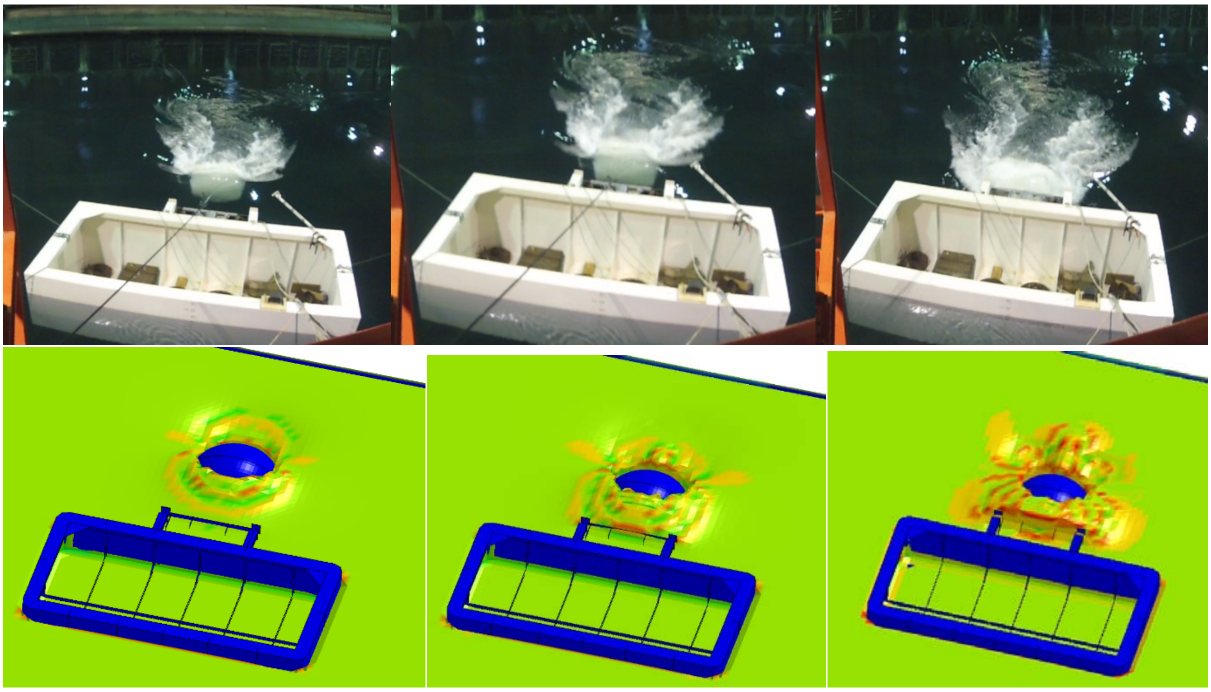

Figure 14. A sequence of images extracted from the video recording of the test (above) and the numerical simulation (below) from the above.

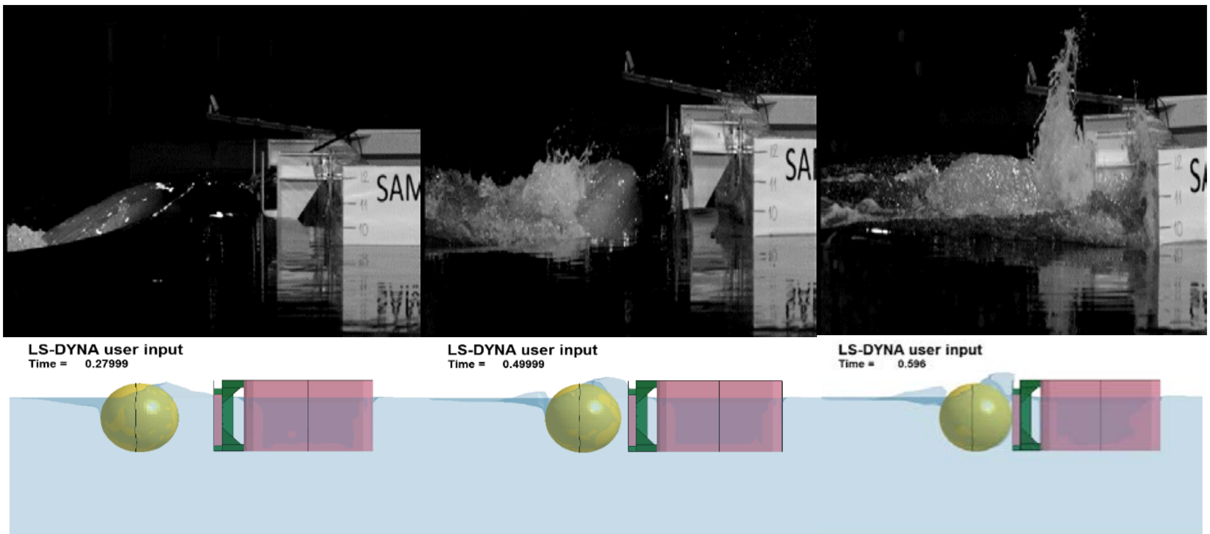

Figure 15. A sequence of images extracted from the HSV of the test (above) and the numerical simulation (below) from the side.

4.2 The CAM method

4.2.1 Simulation setup

Numerical simulations of the ice block's impact with the floater were performed without the fluid model. The floater was assumed to be stationary before the impact, and the initial velocity of the ice block was 2 m/s; these were the same as the initial states in the test. The hydrodynamic effects of the surrounding water were taken into account as constant added masses throughout the collision. Therefore, predicting the velocities of the ice block and the floater before the impact using the CAM method was impossible.

As the duration of the impact in the test was very short, i.e., approximately 22 milliseconds, the added mass coefficients for infinite high frequency can be used [ ]. The value of 0.35 for the ice block and of 0.33 for the floater which were obtained by WADAM (see Figure 11 and 12) were used in the CAM-based simulations.

The numerical model is shown in Figure 16. The material parameters of the floater and the ice block were the same as they were in Section 4.1 except for the density. To maintain the correct energy dissipation, the density of the panel and the front half of the ice were the same as they were in the FSI-based simulations; only the densities of the remaining parts were changed to take the added mass contributions into account. To avoid changing the effect of the element size on the collision response, the size of the elements of both the floater and the ice block were the same as they were in the FSI-based simulation. The total number of elements was much lower in the CAM-based simulation than in the FSI-based simulation due to the absence of water and air. The ice block was meshed with 8-node solid elements with reduced integration and stiffness-based hourglass control, and the floater was meshed with 4-node shell elements. No gravity was applied to the elements in this simulation. The contact between the ice block and the panel and the self-contact of the ice component were implemented the same manner as they were in the FSI-based simulation.

Because the velocities of the ice block and the floater before the impact were changed as a result of the bow wave effect, the case with the “true” velocities at the instant of impact was also investigated. In this case, the velocities of the ice block and the floater were assumed to be 1.8 m/s and 0.1 m/s, respectively, as estimated using the HSV of the test.

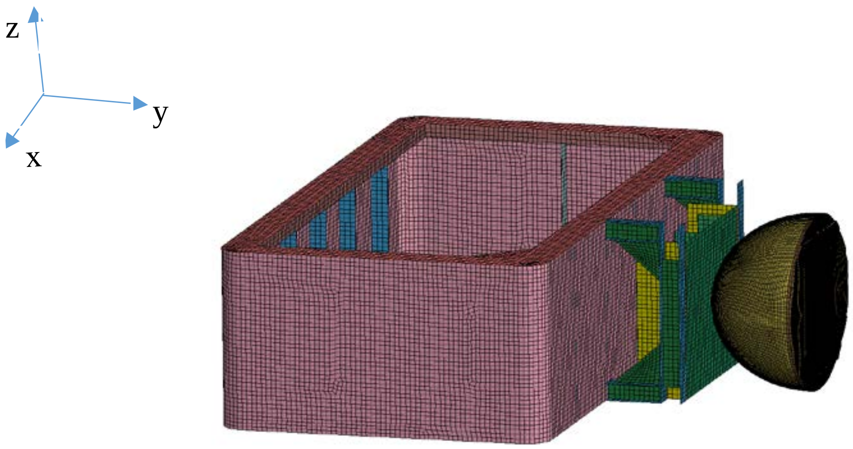

Figure 16. The finite element model of the floater and the ice block.

4.2.2 Results

Figure 17 shows the time histories of the contact forces from the results of CAM-based simulations. The comparison of the results shows that the case with the “initial” velocity predicts a higher peak force than the case with the “true” velocities. In the case with the “initial” velocities, the peak force was 115 kN and the total energy dissipation in the ice block was 1.85 kJ; the corresponding values were 89 kN and 1.34 kJ, respectively, in the case with the “true” velocities. These differences are due to the larger relative velocity between the ice block and the floater in the case with the “initial” velocities. It indicates that the relative velocity before the impact has significant effect on the collision response with respect to the contact force and energy loss.

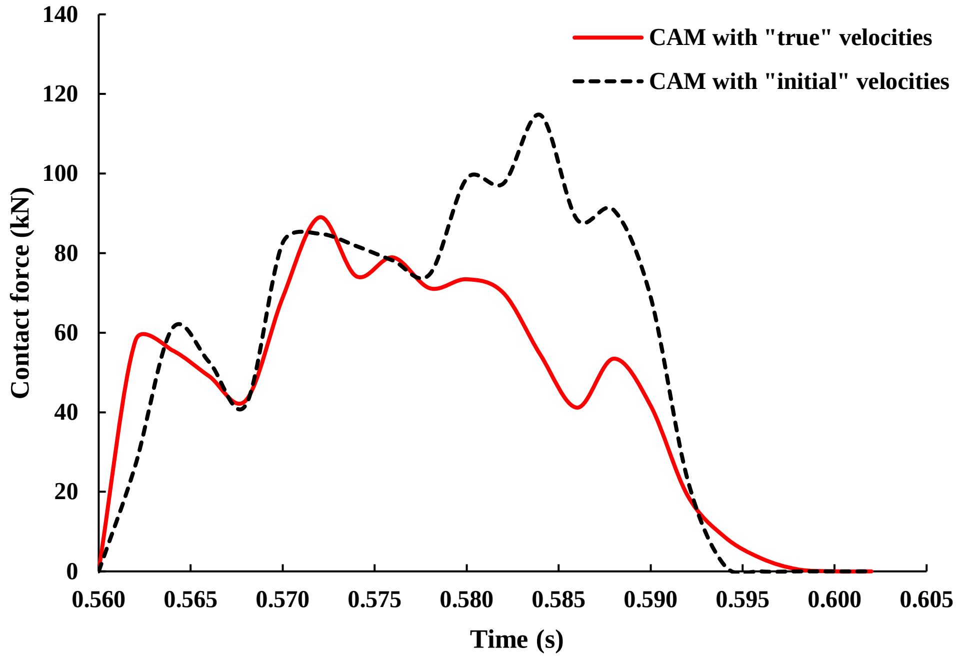

Figure 17. The contact force between the panel and the ice block during the collision versus time.

5. Comparison of the results of the two methods

Comparisons of the results of the FSI method and the results of the CAM method are presented below. They include the acceleration of the floater wall with the DMU on it, the contact force and the total energy dissipation in the ice block and the CPU time. To evaluate the results from two methods, the time history of the acceleration of the floater wall measured by the DMU during the test was used. It is noted that the results of the CAM-based simulation with the “true” velocity (i.e., 1.8 m/s for the ice block and 0.1 m/s for the floater) were used for comparison. All the simulations were run on an 8 CPU workstation with Intel 3.4 GHz processors and 32.0 GB of RAM. The software used was LS-DYNA version Ls971 R5.1.1 revision 65543 with single precision.

5.1 Acceleration of the floater wall with the DMU on it

Figure 18 shows the comparison of the acceleration time histories of the floater wall with the DMU on it from the test and the CAM- and FSI-based simulations. It is noted that the accelerations in the numerical simulations were calculated from the same location as in the test by the DMU (for the location of the DMU see Figure 2).

These histories represent the vibration response of the local plate and indicate that the panel vibrated significantly in the test and the numerical simulations due to the ice block's impact. Both high- and low-frequency components are presented in the registered and simulated responses. As shown in Figure 18, the FSI-based simulation's acceleration time history is almost the same as that of the test in the first 22 milliseconds, i.e., during the initial response to the impact. However, there are slight phase and a little peak differences in the dynamic response of the steel floater after the 22 milliseconds, i.e., during the second vibration phase. These differences may be caused by the limitations of the ALE solver, in which it does not account for the fluid boundary layer effect and the coupling force is a function of the displacement (i.e., see Chapter 2.2). Overall, the FSI-based simulation agrees well with the test. In the initial 22 milliseconds, the maximum acceleration in the CAM-based simulation was 20.8 m/s^2, compared to 21 m/s^2 in the test. This agreement indicates that the CAM method may predict the initial collision response with reasonable accuracy. However, after the 22 milliseconds (see Figure 18), it is clear that the peaks in the results of the CAM-based simulation are significant higher than those in the results of the test. Moreover, in the CAM-based simulation the oscillation period is much smaller than in water, especially during the initial part of the shown evolution. These differences are due to the neglect of the dynamic interactions between the water, the ice block and the floater in the CAM method.

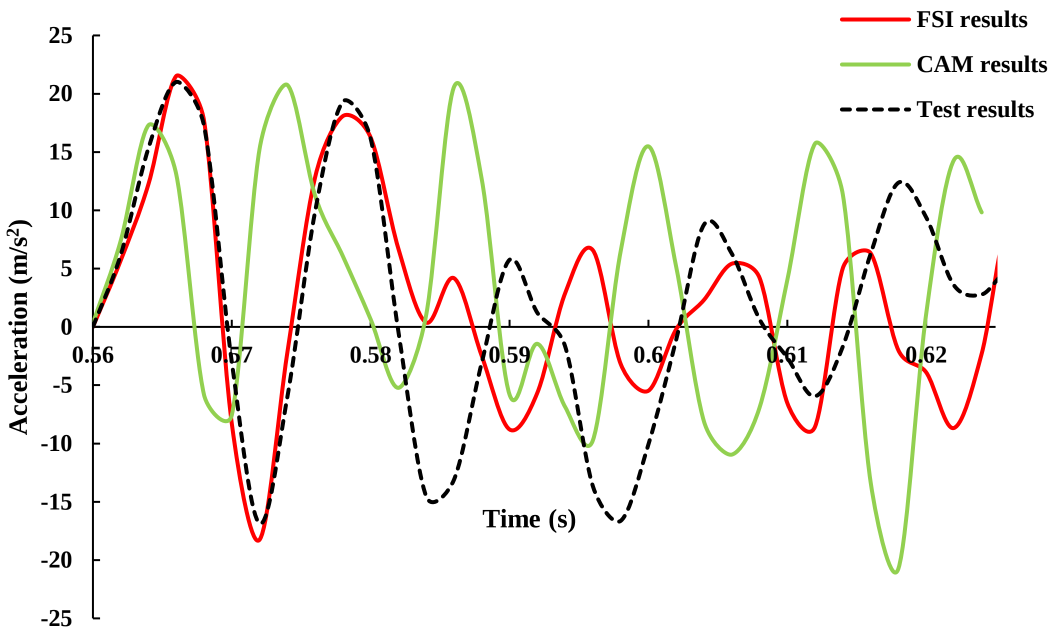

Figure 18. Acceleration of the floater wall with the DMU on it from two simulations and test.

In short, the FSI method with verified ice and water models can provide more realistic and reliable predictions of the collision response of the floater wall with the DMU on it as far as sway accelerations are concerned than the CAM method. However, it has a lower computational efficiency than the CAM method because more elements are added to the model. The details of this will be discussed later. The increased accuracy is due to the better approximation of the hydrodynamic effects during the collision, and the decreased computational efficiency is due to the demands of numerically solving for the fluid's motion.

5.2 Contact force

Figure 19 shows the contact force versus time from the FSI- and CAM-based simulations. The comparison shows that the FSI-based simulation had a lower peak force and a shorter impact duration. The peak force was 74.7 kN in the FSI-based simulation and 89.0 kN in the CAM-based simulation. The duration of the impact in the FSI-based simulation was approximately 28 milliseconds, compared to approximately 38 milliseconds in the CAM-based simulation.

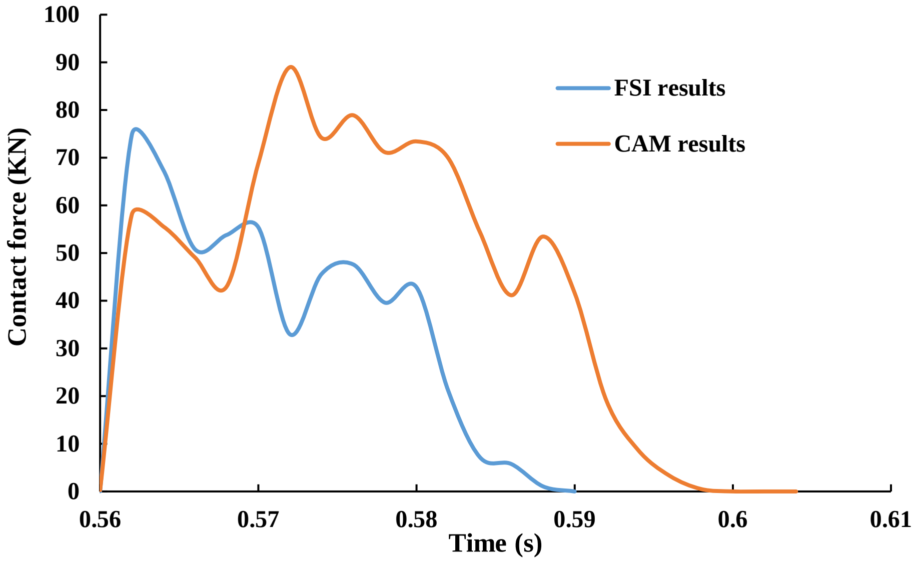

Figure 19. The contact force between the panel and the ice block during the collision versus time.

5.3 Energy dissipated in the ice

Figure 20 shows the time histories of the energy dissipated in the ice block from the FSI- and CAM-based simulations. Figure 21 shows the deformation of the ice block after the impact in the two simulations. It is observed that the ice block was more significantly crushed in the CAM-based simulation than it was in the FSI-based simulation. The CAM-based simulation predicted a greater amount of energy dissipated in the ice block than the FSI-based simulation did. In the CAM-based simulation, the amount of energy dissipated in the ice was 1.34 kJ, compared to 0.91 kJ in the FSI-based simulation. The possible reasons for the difference are the following:

- In the FSI-based simulation, the water was forced out of the general space between the ice and floater both before and during the ice-floater contact. Before contact the floater was pushed by the water (i.e. the bow wave of the ice) as the ice movement effectively reducing the relative impact velocity. The displaced water and the forced movement of the floater by the water both dissipated portions of the energy, whereas there was no energy dissipation in the CAM-based simulation before contact took place. These energy-dissipation effects continued to happen in the FSI-based simulation, even after ice-floater contact initiates, right up until the ice penetration reached its maximum value.

- Due to the hydrodynamic interaction between the bodies, the sway added mass may differ from that calculated for the bodies separately for infinite high frequency. The values of the constant added mass that were assumed in the CAM-based simulations may overestimate the hydrodynamic effect and therefore, caused the amount of energy dissipated in the ice block to be overestimated.

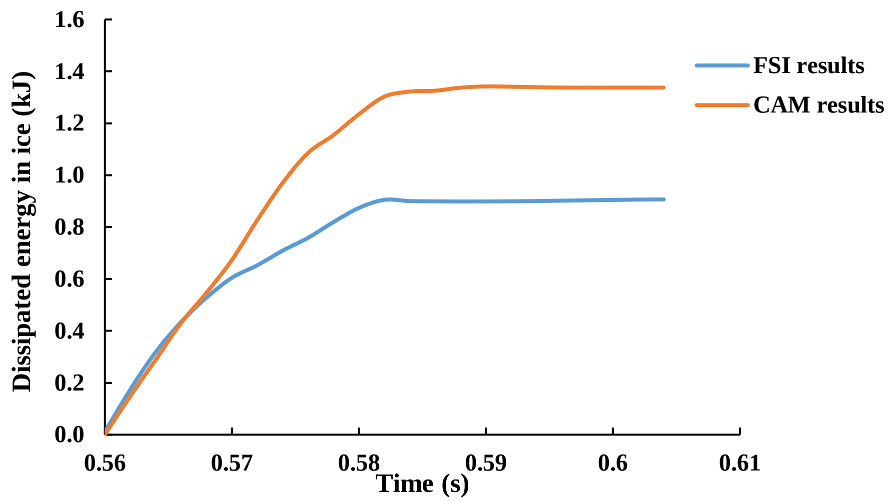

Figure 20. The amount of energy dissipated in the ice block versus time.

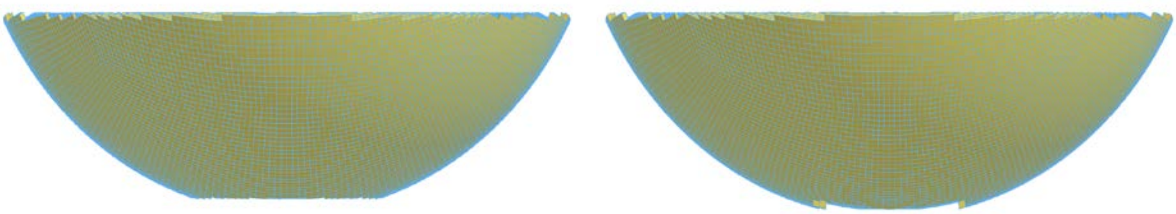

(a) (b)

Figure 21. The deformation of the ice block after the impact: (a) CAM-based simulation; (b) FSI-based simulation.

In summary, by comparing the results of the FSI- and CAM-based simulations (described in Sections 3 and 4), it is concluded that the surrounding water has a noteworthy effect on the motions of the ice block and the floater when they are close and therefore, affects the collision response of the floater, the contact force history and the energy dissipation.

5.4 CPU time

The number of elements and the timing information from the two methods are presented in Table 3. The total number of elements was 40% greater in the FSI-based simulation than it was in the CAM-based simulation. The calculation time and the total CPU time were one order of magnitude larger in the FSI-based simulation. This shows that the CAM method sped up the calculation significantly.

It is noted that workstations with larger numbers of CPUs are currently available. In addition, massively parallel processing (MPP) is a type of computing available for LS-DYNA that uses many separate CPUs running in parallel. Each CPU has its own memory and executes a single analysis. Consequently, simulations such as the present two can be run in much shorter time periods. Therefore, the CPU times given in the table should only be considered comparative values; they are not absolute.

Table 3. Comparison of the CPU time*

Method	Number of elements	Simulation time (s)	CPU time (h)
FSI	1904200	0.63	248
CAM	1424200	0.07	20

*The CPU times listed in the table should only be considered comparative values; they are not absolute. The reason is that the simulations can run in much shorter time if a workstation with more CPUs and/or massively parallel processing (MPP) solvers are used.

6. Discussion

The objective was to compare the CAM and FSI methods. To do so, we used the FSI and CAM methods to analyse the ice-structure interaction problem of a collision between a freshwater ice block and a movable structure. Our results confirm that the FSI method can provide more realistic and accurate predictions of the responses of the ice and the structure than the CAM method can, as long as ice's behaviour and the fluid model are adequately verified. There was good agreement between the results of the FSI-based simulation and the experimental data with regard to the sway acceleration of the floater wall with the DMU on it. The CAM method was able to predict the initial response of the floater (i.e., the maximum sway acceleration) quite well during the first 22 milliseconds, but overestimated the peak contact force, the impact duration and the amount of energy dissipated in the ice block. These results and their applicability are discussed in the following paragraphs.

The validation of LS-DYNA's fluid model in this study (see Section 3.1.3) is similar to the transient approach used by Zong [28]. The sway added mass determined using a force vibration analysis was found to be virtually independent of the magnitude of the applied force, which confirmed the results obtained by Zong [28].

The relative velocity between the ice and the floater before the impact was influenced noticeably by the hydrodynamic interaction between the ice and the floater (the "bow wave"). It was 1.73 m/s in the FSI-based simulation and 1.70 m/s in the experiment. The results demonstrated that the FSI method is capable of simulating this bow wave effect accurately.

In contrast to the FSI method, the CAM approach cannot predict changes in the velocities of the ice block and the floater prior to impact. When their hydrodynamic interaction were not taken into account, the CAM-based simulation overestimated the peak contact force and the amount of energy dissipated in the ice block. This is because the relative velocity between the ice block and the floater immediately before the impact was greater than it was in the test.

The acceleration histories of the floater wall with the DMU on it in the FSI-based simulation and the test (shown in Figure 14) agreed quite well in terms of magnitude and frequency. This agreement between the experimental and numerical results indicates that the FSI method can accurately predict the response of the floater. This finding is similar to the FSI-based model's prediction of the acceleration response of a lifeboat in free-fall described by Bae and Zakki [29]. When the measured velocities were used in CAM-based simulations, the maximum accelerations of the floater wall compared reasonably well with the experimental data. However, after the first 22 milliseconds (see Figure 16), the accuracy of its prediction of the collision response during the free vibration phase was lower.

The comparison between the FSI- and CAM-based simulations in Section 5 also shows that the CAM method estimated a higher peak force during the impact, a longer impact duration and a larger amount of energy dissipated in the ice block. These differences may be caused by the effect of the hydrodynamic interaction between the two bodies on the sway added mass of the ice block. When two bodies are close to each other, the sway added mass of each body can be divided into two parts due to the hydrodynamic interaction. One part is induced by the sway mode of the body itself, and the other is induced by the sway mode of the other body. Besides, the bow wave between the ice block and the floater was observed in both FSI-based simulation and test. As the size and mass of the ice block was smaller than the floater, this wave should have more influence on the sway acceleration of the ice block and thus affect the sway added mass of the ice block. If a smaller added mass coefficient for the ice block was used in the CAM method, we can expect that the peak accelerations of the floater wall with the DMU on it after the 22 milliseconds will reduce (i.e., closer to the values in the test) and peak force and energy dissipated in the ice block will be closer to the values estimated in the FSI-based simulation. It indicates that the added mass coefficient for the ice block related to the forward motion may be small in this case. Therefore, for the case that the hydrodynamic interaction has significant effect on the motions of the impact bodies before the impact, the added mass coefficient values should be careful evaluated for the CAM-based simulation. For the ship-ship collision, in the most case the bow wave induced by the forward motion of the colliding ship is small due to the effective shape of ship bow and thus has little effect on the motions of two ships when they are close. The added mass coefficient related to the forward motion of the ship has been found to be 0.02 to 0.07[ ]. The sway added mass coefficient for the collided ship has been taken as 0.4 [ ]. Thus, if the duration of the impact is very short, the CAM-based simulation using these added mass coefficients may provide similar results compared with the FSI-based simulation for ship-ship collision.

Both the FSI- and CAM-based simulations predicted that the structure was sufficiently strong to crush the ice block with no permanent deformation of the impacted plate. This was confirmed by the experimental test.

The computational efficiency of the CAM method was one order of magnitude better than that of the FSI method. This was partly due to the number of finite elements, which was 40% larger in the FSI-based simulation, in which the water and air were also modelled. However, the computation time increased significantly by more than the sheer number of elements. This was because several factors contributed to the increase in CPU time. These were: (1) the time-consuming solution in the fluid domain; (2) the FSI method must simulate the ice moving towards the floater to generate the hydrodynamic interaction during the approach phase; (3) the ALE formulation used to solve the FSI problem was relatively expensive in comparison with the Lagrangian approach because of the additional advection, interface reconstruction, and coupling computation [23].

Regarding the numerical discretization, both the FSI- and CAM-based simulations required fine meshes for the regions of the ice and the panel where the two objects came into contact during the collision. The simulation results (the peak force) were sensitive to the size of the elements on the ice block and the floater (see Figure and Figure). This finding is similar to that for collisions between ice and stiffened panels (see Kim et al. [3] for details). In addition, there are practical limitations on how small the elements in a CAM- or FSI-based simulation can be because the simulation's time step is determined by the size of the smallest element in the mesh. Furthermore, if all the elements are small, then a large number of them is involved in the computations, which leads to an extremely large amount of CPU time. Consequently, to obtain accurate results, the size of the elements on the ice block and the floater should be carefully evaluated prior to performing FSI- or CAM-based simulations. Studying the sensitivity of the element size and other important parameters such as the fluid viscosity and the equation of state used in the water model have been carried out [ ].

In this study, we have performed FSI-based simulations of a collision between an 850 kg laboratory-grown freshwater ice block and a 7537 kg steel structure. In a full-scale scenario (e.g., a collision between a stationary vessel and a bergy bit), the ice block and the impacted structure may be larger and have different shapes. In addition, the numerical discretization will differ from the one used in this study. ALE-based simulations of full-scale ship-ice collisions with realistic ice shapes and verified constitutive ice models are rarely performed, and currently, there is not enough experimental and/or numerical data to further discuss how the hydrodynamic interaction influences the collision response in the full-scale scenario. In the future, we will use the FSI method to analyse full-scale ship-ice collisions.

7. Summary and conclusions

Numerical simulations of an impact between an ice block and a deformable steel floater have been performed using two methods: the FSI method and the CAM method. To ensure reliable results, validation of the ice and fluid models in LS-DYNA were performed. The results of the FSI- and CAM-based simulations were compared with experimental results, notably with respect to the acceleration of the floater wall with the DMU on it, the contact force, and the amount of energy dissipated in the ice block and the CPU time. The major findings are summarized as follows:

- The FSI method can provide more realistic and reliable predictions of the floater wall's acceleration history than the CAM method can for the problem of a collision between an ice block and a floating steel structure. The accelerations calculated using the FSI method agree reasonably well with the acceleration time history measured in the ice-structure collision experiments. Besides, there is a good agreement between the FSI-based simulation and the test with respect to the phenomena (i.e., bow wave) and the relative velocity between the ice block and the floater before the impact.
- The maximum acceleration in the CAM-based simulation compares reasonably well with that of the test during the initial response to the impact. The accuracy of its prediction of the collision response during the second vibration phase (i.e., after the 22 milliseconds) is somewhat worse. In addition, the CAM-based simulation cannot predict the "true" velocities of the ice block and the floater immediately before the impact because it neglects the hydrodynamic interaction during the approach phase. Using the "undisturbed" initial velocities causes it to overestimate the contact force and the amount of energy dissipated in the ice block.
- Compared with the results of the FSI-based simulation, the CAM-based simulation estimates a higher peak force, a longer impact duration and a greater amount of energy dissipated in the ice block.
- The CAM method is simple to use and much more computationally efficient than the FSI method is. This is mainly due to its omission of the fluid model.

Acknowlegements

The authors would like to thank the Norwegian University of Science and Technology (NTNU) and the China Scholarship Council (CSC). This work was supported in part by the

Research Council of Norway through the Centre of Excellence funding scheme, project AMOS (project number 223254), and through the Centre of Research-based Innovation scheme, project SAMCoT (project number 203471).

References

[1] IACS. Unified Requirements Polar Class, International Association of Classification Societies; 2011.

[2] DNV GL. Rules for Classification of Ships. Ships for Navigation in Ice. Det Norske Veritas; 2011.

[3] Han S., Lee J.Y., Park Y.I. and Che J. Structural risk analysis of an NO96 membrane-type liquefied natural gas carrier in Baltic ice operation. Journal of Engineering for the Maritime Environment 2008; 222: 179-194.

[4] Daley C. and Kim H. Ice collision forces considering structural deformation. Proceedings of ASME 29th International Conference on Ocean, Offshore and Arctic Engineering (OMAE2010); Paper OMAE2010-20657.

[5] Gagnon R. Physical model experiments to assess the hydrodynamic interaction between floating glacial ice masses and a transiting tanker. Journal of Offshore Mechanics and Arctic Engineering 2004; 126(4): 297-309.

[6] Lee S.G., Nam J.H., Kim J.K., Zhao T. and Nguyen H.A. Structural safety assessment of ship collision using FSI analysis technique. Proceedings of the Twenty-second International Offshore and Polar Engineering Conference 2012; June 17-22.

[7] Motora S., Fujino M. and Sugiura M. Equivalent added mass of ships in collisions. Selected Papers from the Journal of the Society of Naval Architects of Japan, 1971; 7: 138-148.

[8] LSTC. LS-DYNA User's Manual, Version 971 R5, Livermore Soft Technology Corp., USA; 2011.

[9] Minorsky, V.U. An analysis of ship collision with reference to protection of nuclear powered plants. Journal of Ship Research 1959; 3(2): 1-4.

[10] Wang Z.L., Jiang Z.Y. and Gu Y.N. An added mass model for numerical simulation of ship/ ship collisions. Explosion and shock waves 2002; 22(4); 321-326.

[11] Kim E., Storheim M., von Bock und Polach R.U.F. and Amdahl, J. Design and modeling of accidental ship collisions with ice masses at laboratory scale. Proceedings of the 31st International Conference on Ocean Offshore and Arctic Engineering, 2012; 495-506.

[12] Pedersen P.T. and Zhang S. On impact mechanics in ship collisions. Marine Structure 1998; 11(10): 429-449.

[13] Yamada Y. and Pedersen P. T. Simplified analysis tool for ship-ship collision. Proceedings of the Seventeenth International Offshore and Polar Engineering Conference, ISOPE 2007; 3760-3764.

[14] Yang P. D. C. and Caldwell J. B. Collision energy absorption of ship's bow structures. Int. J. Impact Energy 1988; 7(2): 181-196.

[15] Kim, E., Storheim, M., Løset, S. and von Bock und Polach, R.U.F. Laboratory experiments on shared-energy collisions between freshwater ice blocks and a floating steel structure, 2015 (in preparation).

[16] Kwak M.J., Choi J.H., Park J.H. and Woo J.H. Strength assessment for bow structure of arctic tanker under ship-ice interaction. Daewoo Shipbuilding and Marine Engineering Co., LTD, RINA ICSOT 2009.
[17] Zhang A. and Suzuki K. Numerical simulation of fluid-structure interaction of liquid cargo filled tank during ship collision using the ALE finite element method. International Journal of Crashworthiness 2006; 11(4): 291-298.
[18] Campana E. F., Peri D., Tahara Y. and Stern F. Shape optimization in ship hydrodynamics using computational fluid dynamics. Computer Methods in Applied Mechanics and Engineering, 2006; 196(1-3): 634-651.
[19] Song M., Kim E. and Amdahl J. Fluid-structure-interaction analysis of an ice block-structure collision. Proc. 23rd International Conference on Port and Ocean Engineering under Arctic Conditions, Trondheim, Norway, 2015.
[20] Smith C. and Stojko S. The application of fluid structure interaction techniques within finite element analyses of water-filled transport flasks. 14th International Symposium on the Packaging and Transportation of Radioactive Materials, 2004; 214-222.
[21] Yu Z.L., Amdahl J. and Storheim M. A new approach for coupling external dynamics and internal mechanics in ship collisions. Marine Structures 2015; 45: 110-132.
[22] Derradji-Aouat A. and Gavin J. Earle. Ship-Structure Collision: Development of a numerical model for direct impact simulations. In: Proceedings of the Thirteenth International Offshore and Polar Engineering Conference, Honolulu, Hawaii, USA, 2003; 520- 527.
[23] Lee, S.G. and Nguyen, H.A. LNGC collision response analysis with iceberg considering surrounding seawater. Proceedings of the 20th International Offshore and Polar Engineering Conference, Beijing, China, ISHOPE, 2010; 3: 206-214.
[24] Wang J.Y. and Derradji-Aouat A. Ship performance in broken ice floes-Preliminary numerical simulations. Institute for Ocean Technology, National Research Council, St. John’s, NL, Canada, Report No. TR-2010-24.
[25] Gagnon R. and Derradji-Aouat A. First results of numerical simulations of bergy bit collision with the CCGS terry fox icebreaker, the 18th International Symposium on Ice, Sapporo, Japan; 2006.
[26] Gagnon, R. and Wang J. Numerical simulations of a tanker collision with a bergy bit incorporating hydrodynamics, a validated ice model and damage to the vessel. Cold Region Science and Technology 2012; 81(26-35).
[27] Ulan-Kvitberg C., Kim H. and Daley C. Comparison of pressure-area effects for various ice and steel indenters. Proceedings of the 2011 International Offshore and Polar Engineering Conference, Maui, Hawaii, USA, 2011; 1048-1055.
[28] Oldford D. Sopper, R. and Daley C. Impact ice loads on spherical geometries. ICETECH14-120-RF, Proceedings of ICETECH2014 conference, July 28-31, Banff, Alberta, Canada; 2014.
[29] Storheim M., Nord T., Kim E., Høyland K., Langseth M., Amdahl J. and Løset S. Pilot study of ice-structure interaction in a pendulum accelerator. Proceeding of the 23rd International Conference on Port and Ocean Engineering under Arctic Conditions, Trondheim, Norway, June 14-18; 2015.
[30] Masterson D.M. and Frederking R.M.W. Local contact pressures in ship/ice and structure/ice interactions. Cold Regions Science and Technology 1993; 21(2): 169-155.
[31] Day J. Guidelines for ale modeling in ls-dyna. Draft; 2010.

[32] Liu, Z., Amdahl, J. and Løset, S. Plasticity based material modelling of ice and its application to ship-iceberg impacts. Cold Regions Science and Technology 2011; 65(3): 326-334.

[33] Alsos, H. S., Amdahl, J. and Hopperstad, O. S. On the resistance to penetration of stiffened plates, Part II: Numerical analysis. International Journal of Impact Engineering 2009; 36: 875-887.

[34] Bass D. and Sen D. Added mass and damping coefficient for certain “realistic” iceberg models. Cold Regions Science and Technology 1986; 12(2): 163-174.

[35] Petersen, M.J. and Pedersen, T. Collision between ships and offshore platforms. Proceedings of the Offshore Technology Conference, 1981;. 163-172.

[36] Zong R. Finite element analysis of ship-ice collision using LS-DYNA. Master thesis, Faculty of Engineering and Applied Science, Memorial University of Newfoundland, Newfoundland, Canada, 2012.

[37] Bae, D. M. and Zakki, A. Comparisons of Multi material ALE and single material ALE in LS-DYNA for estimation of acceleration response of free-fall lifeboat. Journal of the Society of Naval Architects of Korea 2011; 48(6): 552-559.